Temporal analysis of nonresonant two-photon coherent control involving bound and dissociative molecular states

Jing Su, Shaohao Chen,* Agnieszka Jaroń-Becker, and Andreas Becker
JILA and Department of Physics, University of Colorado, Boulder, Colorado 80309, USA
(Received 3 October 2011; published 8 December 2011)

We theoretically study the control of two-photon excitation to bound and dissociative states in a molecule induced by trains of laser pulses, which are equivalent to certain sets of spectral phase modulated pulses. To this end, we solve the time-dependent Schrödinger equation for the interaction of molecular model systems with an external intense laser field. Our numerical results for the temporal evolution of the population in the excited states show that, in the case of an excited dissociative state, control schemes, previously validated for the atomic case, fail due to the coupling of electronic and nuclear motion. In contrast, for excitation to bound states the two-photon excitation probability is controlled via the time delay and the carrier-envelope phase difference between two consecutive pulses in the train.

DOI: 10.1103/PhysRevA.84.065402 PACS number(s): 33.80.Rv, 33.80.Wz

Initial ideas of quantum coherent control were based on quantum path interferences using phase-controlled laser fields [1] and pump-dump (pump-probe) schemes using sequences of laser pulses with tunable delays [2,3]. At first glance the former technique makes use of coherence properties of light fields in the frequency domain while the latter takes advantage of the temporal evolution of a process. However, converting the respective analysis from one domain to the other often adds a complementary view on a particular control scheme [4]. Recent development of femtosecond pulse shaping techniques extended the variety of schemes in quantum coherent control (for a review, see Ref. [5]), which is often analyzed in the frequency domain based on the multipathway interference concept. For example, destructive and constructive interference among various pathways can tune few-photon absorption probabilities to zero or maximum by modification of the spectral phase of the pulse (e.g., [6–10]). We recently investigated some of these control schemes based on spectral phase modulations from the complementary time-dependent perspective via numerical solutions of the time-dependent Schrödinger equation (TDSE) of an atom [11]. The analysis showed that two-photon excitation probabilities in an (hydrogen) atom are controlled via destructive or constructive interferences between the amplitudes induced by consecutive subpulses in a pulse train. The results also provided insights into the control of atomic $(2+1)$-photon ionization processes. Here, we supplement our previous studies by the time-dependent analysis of the control of different types of two-photon transitions in molecules, namely, bound-to-bound state and bound-to-dissociative state transitions.

To this end, we make use of two models describing the interaction of a single-active-electron diatomic molecule with an external field. The following two-dimensional (2D) model, which accounts for the coupled electronic and nuclear dynamics, has been frequently applied in simulations of H_2^+ interacting with a laser field. The field-free Hamiltonian is given by (we use Hartree atomic units, $e = m = \hbar = 1$, if not specified otherwise)

$$H_1(R,z) = \frac{p_R^2}{2M} + \frac{p_z^2}{2m} - \frac{1}{\sqrt{(z+R/2)^2+a_1}} - \frac{1}{\sqrt{(z-R/2)^2+a_2}} + \frac{1}{\sqrt{R^2+b}}, \quad (1)$$

where M and m are the reduced masses of the nuclei and the electron, respectively. R is the internuclear distance, z is the electron position with respect to the center of mass of the nuclei, and a_1 and a_2 as well as b are soft-core Coulomb parameters. In the case of H_2^+ one chooses $a_1 = a_2$. However, the symmetry of the corresponding Hamiltonian prohibits a two-photon transition from the electronic ground state to the first dissociative state.

For our goal to study the coherent control of two-photon processes we set $a_1 \neq a_2$ to break the symmetry of the Hamiltonian. In our studies, we arbitrarily choose $a_1 = 1.0$, $a_2 = 2.0$, and $b = 0.03$. The adiabatic potential energy curves for the ground and first excited state of this system, calculated using imaginary time propagation of the corresponding Schrödinger equation, are shown in Fig. 1(a). The equilibrium distance of the two protons is $R_0 = 3.36$, and the energy gap between the states at R_0 is $\Delta E = 6.88$ eV. The curve of the first excited state has a shallow well, which however does not influence the dissociative character of the state for wave packets pumped from the initial ground state close to the equilibrium distance.

To study transitions between bound states, we make use of a molecular model system in which the Coulomb repulsion $1/R$ is replaced by a Morse potential:

$$H_2(R,z) = \frac{p_R^2}{2M} + \frac{p_z^2}{2m} - \frac{1}{\sqrt{(z+R/2)^2+a_1}} - \frac{1}{\sqrt{(z-R/2)^2+a_2}} + \mathcal{D}(1-e^{-\lambda(R-R_0)})^2 - \mathcal{D}, \quad (2)$$

where $\mathcal{D}$ is the depth of the well, R_0 is the equilibrium distance, $\lambda = \sqrt{k/2\mathcal{D}}$ with k being the bond force constant, and all the

*Present address: Department of Physics and Astronomy, Louisiana State University, Baton Rouge, LA 70803-4001, USA.

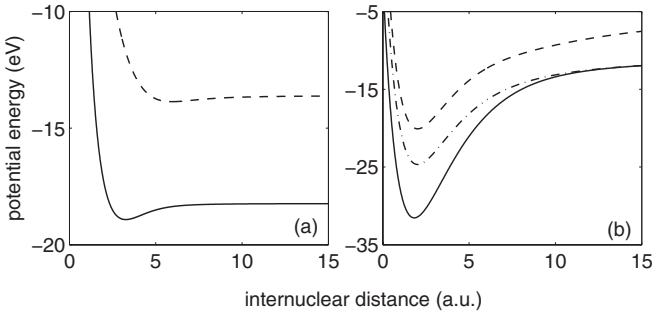

FIG. 1. Potential energy curves of the ground and lowest lying excited states of our 2D molecular model systems: (a) model with a dissociative excited state and (b) model with bound excited states.

other parameters are defined as before. Using $a_1 = a_2 = 4.0$, $\mathcal{D} = 0.4$, $\lambda = 0.5$, and $R_0 = 2.0$, the potential energy curves of the ground state and the first two excited states, shown in Fig. 1(b), are well separated. We consider nonresonant two-photon transitions to the second excited state, which is possible since the energy difference between the ground state and the first excited state clearly exceeds the corresponding photon energy required for the two-photon transition.

To investigate the time evolution of the excitation process, we solve the corresponding TDSE of the molecular model systems interacting with a laser pulse linearly polarized along the internuclear axis ($j = 1,2$),

$$i\frac{\partial}{\partial t}\Phi(R,z;t) = [H_j(R,z) + E(t)z]\Phi(R,z;t), \qquad (3)$$

in a grid representation using the Crank-Nicholson method. For the field interaction we use dipole approximation and the length gauge. To discretize the partial differential equation, we employ a time step of $\Delta t = 0.01$ and a spatial grid with spacings of $\Delta R = 0.03$ and $\Delta z = 0.2$. The populations in the ground state and the excited bound states are obtained by projection on the respective field-free states, which for the laser parameters used in the present study is a reasonable approximation even during the interaction with the external field. In the case of the excited dissociative state the population is calculated as $P_{\rm exc} = 1 - \sum_{\nu=0}^{n} P_\nu$, where ν denotes the vibrational mode in the electronic ground state and n is the total number of the vibrational states considered. The ionization and dissociation probabilities are calculated as the outgoing probability flux at the respective boundaries of the grid. At the edges we use $\cos^{1/6}$ mask functions to suppress reflections. We have checked that the results are not influenced by the remaining small inaccuracies due to the boundary conditions. We use a grid of $N_R \times N_z = 600 \times 200$ points ($N_R \times N_z = 400 \times 600$ points) for the dissociative (bound) state model.

First, we investigate control of two-photon excitation from a bound state to a dissociative molecular state. To this end, we consider the dissociative state model and a spectral phase modulated laser electric field of the form

$$E\left(\frac{\omega}{2} + \Omega\right) = E_0 \mathrm{sech}\left(\frac{1.76\Omega}{\Delta\omega}\right) \exp[i\alpha\cos(\beta\Omega + \phi)]. \qquad (4)$$

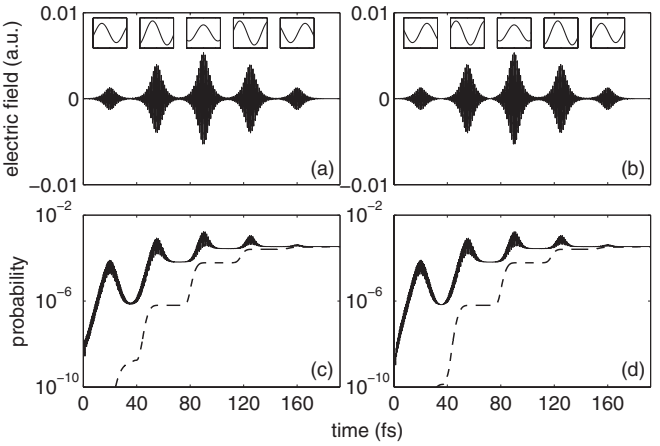

FIG. 2. Two-photon coherent control to a dissociative molecular state. The upper panels show the electric field distribution as a function of time for (a) $\phi = 0$ and (b) $\phi = \pi/2$. The insets show the central field cycle and the carrier-envelope phase of each subpulse. In the lower panels the time evolution of the probabilities in the first excited state (solid line) is presented for (c) $\phi = 0$ and (d) $\phi = \pi/2$. We also show the dissociation probabilities (dashed line).

Such fields have been used recently by Meshulach and Silberberg [6] to study the control of two-photon transitions in atoms. For our numerical simulations we choose the central frequency $\omega/2 = 3.44$ eV (half of the energy gap of the desired transition), the bandwidth $\Delta\omega = 0.2$ eV, the modulation depth $\alpha = 1.2024$, and the modulation frequency $\beta = 35$ fs, while the modulation phase ϕ is varied. A Fourier transform (FT) of these fields yields a pulse train in the temporal domain. In our studies we fix the (overall) peak intensity in the pulse train to $I_0 = 1 \times 10^{12}$ W/cm^2, which for the present frequencies is within the perturbation regime.

In the atomic case it was shown [12] that using $\phi = 0$ a dark pulse is formed and the final population in the excited state vanishes. On the other hand the excitation probability was found to be maximized for $\phi = \pi/2$. In contrast, we find that for the two-photon transition to a dissociative state in the present molecular model system that the final excitation probability is independent of the specific value of ϕ, as exemplified by the results for $\phi = 0$ (left-hand panels) and $\pi/2$ (right-hand panels) in Fig. 2. The excitation probability increases stepwise with the interaction of every subpulse and equals the probability for dissociation at the end (dashed lines). This indicates that it is the nuclear dynamics which causes the breakdown of the coherent control scheme.

In order to confirm this assumption, we perform another series of calculations in which we fix the internuclear distance $R = R_0$ in Eq. (1) to suppress any nuclear dynamics but keep all other parameters unchanged except the central frequency $\omega/2 = 3.48$ eV. The central frequency is slightly increased since the ground state energy of the fixed nuclei model is lower than that of the 2D model. The results of the fixed nuclei model for $\phi = 0$ (Fig. 3, left-hand panels) and $\phi = \pi/2$ (Fig. 3, right-hand panels) agree with the findings for the atomic case. For $\phi = 0$ the final excited population is (close to) zero (dark pulse), while for $\phi = \pi/2$ the population is maximized (bright pulse). Thus, from the temporal analysis of the process we conclude that coherent control of the two-photon excitation

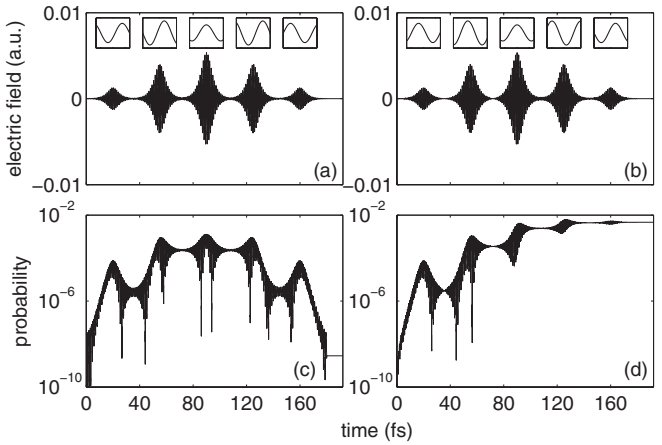

FIG. 3. Same as Fig. 2, but for a molecular model system with fixed internuclear distance $R = R_0$.

to a dissociative molecular state using a train of pulses [or, a spectral phase modulated pulse of the form given in Eq. (4)] fails since each of the wave packets pumped to the excited state by the subpulses in the train quickly propagates to larger internuclear distances. Therefore, concerning the control of the total population in the excited (dissociative) state there is no signature of destructive nor constructive interferences between the wave packets generated from subsequent pulses.

To further study the influence of the relative carrier-envelope phase (CEP) and the time delay between two subpulses on the dissociating nuclear wave packets, we perform a FT to obtain the nuclear momentum distribution. In order to keep the wave packets on the grid up to the end of the simulation, for this analysis we use sets of just two Gaussian subpulses. In Fig. 4(a) we show the momentum spectra for $\tau = 21.0471$ fs and $\phi_{\rm rel} = 0$ as well as $\pi/2$. The spectra are modulated with a period which is inversely proportional to the time delay τ between the pulses. In Fig. 4(b) we present the time delays, extracted from the momentum distributions (circles), and the relative errors to the actual values (stars) as a function of the actual time delays as used in a series of simulations.

Next, we investigate the influence of nuclear dynamics on the control of two-photon excitations to bound molecular

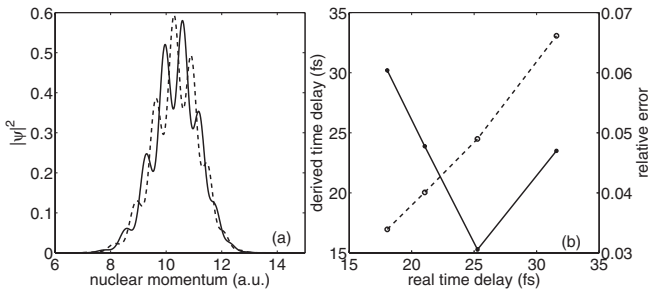

FIG. 4. Momentum analysis of the dissociative wave packets induced by two Gaussian pulses. (a) Nuclear momentum distribution for two different relative CEPs: $\phi_{\rm rel} = 0$ (solid line) and $\phi_{\rm rel} = \pi/2$ (dashed line). (b) Extracted time delay as a function of the actual time delay (circles and dashed line) and relative error between them (stars and solid line).

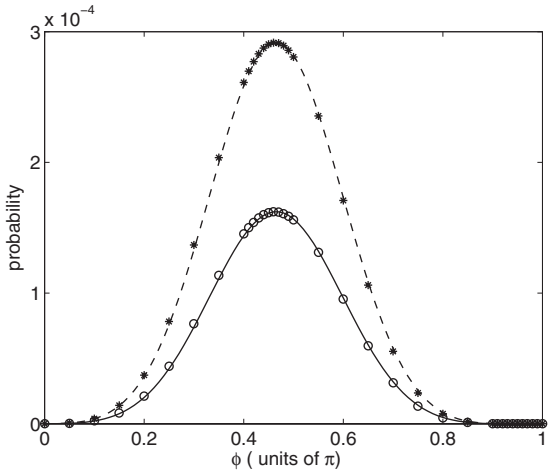

FIG. 5. Excitation probabilities to the ground vibrational state ($\nu_{\rm 2nd} = 0$, circles and solid line) and the first excited vibrational state ($\nu_{\rm 2nd} = 1$, stars and dashed line) as functions of ϕ. A spectral phase modulated field defined in Eq. (4) is used with the following parameters: $\alpha = 1.2024$, $\beta = 8T_{\rm revival} = 85.6682$ fs, $\omega/2 = 5.83$ eV, $\Delta\omega = 0.1$ eV, and $I_0 = 1 \times 10^{11}$ W/cm^2. The symbols (circles and stars) are numerical results obtained by solving the time-dependent Schrödinger equation, while the curves (solid and dashed lines) are obtained using second-order perturbation theory.

states. As shown above, this dynamics becomes effective for the present control scheme over the time delay between two subsequent pulses in a pulse train, since the fundamental control mechanism is based on the interference between two electronic wave packets induced by consecutive subpulses. It is well known from studies in wave-packet interferometry [13,14] that, in the case of a two-pulse scenario, a control of

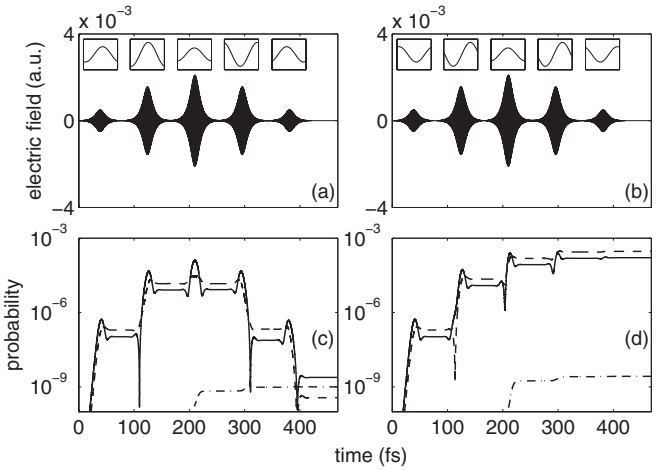

FIG. 6. Two-photon coherent control to a superposition of two vibrational states. The upper panels show that the electric field distribution as a function of time [i.e., the Fourier transform of Eq. (4)] for (a) $\phi = 0.96\pi$ (dark pulse) and (b) $\phi = 0.46\pi$ (bright pulse). The insets show the central field cycle and the CEP of each subpulse. In the lower panels the time evolution of the probabilities in the ground vibrational state (solid line) and the first excited (dashed line) vibrational state is presented for the (c) dark and (d) bright pulses, respectively. Also shown is the ionization probability (dashed-dotted line).

the excitation probability can be achieved via the pulse delay τ and the relative phase ϕ_{rel} of the two pulses. For example, the effective coherent control of the excitation of a superposition of two vibrational states requires $\tau = N\frac{2\pi}{E_{21}-E_{20}} = NT_{\text{revival}}$ and varying ϕ_{rel}. Here, E_{2i} is the energy of the ith vibrational level of the second excited electronic state of our model. The time delays have to coincide with the multiples of the revival period T_{revival} of the vibrational wave packet created in the excited electronic state. This enables the control via efficient interference of wave packets generated by subsequent pulses, since the contributions in both vibrational levels of the second excited electronic state are in phase at these times.

The above analysis for the two-pulse sequence can be readily applied to the spectral phase modulated fields used by Meshulach and Silberberg [6] by noting that the modulation frequency β in Eq. (4) corresponds to the time delay τ between the consecutive pulses in the train in the temporal domain. Furthermore, the relative phase ϕ_{rel} between the consecutive pulses is determined by the modulation phase ϕ in Eq. (4). Thus, setting $\beta = NT_{\text{revival}}$ we expect to achieve an efficient control pattern by changing ϕ. To test our expectations, we do simulations by choosing $\alpha = 1.2024$, $\beta = 8T_{\text{revival}} = 85.6682$ fs, $\omega/2 = 5.83$ eV, $\Delta\omega = 0.1$ eV, and $I_0 = 1 \times 10^{11}$ W/cm^2. Note that we have chosen such a narrow bandwidth that only the lowest two vibrational levels of the second electronic state can be excited. The results of the simulations for excitation to these two vibrational states as a function of the modulation phase ϕ are shown in Fig. 5. The same dependence of the two excitation probabilities on ϕ clearly confirms our expectations. We also show results calculated from the second-order perturbation theory (solid lines) in Fig. 5. Although the coefficient of the transition amplitude [6,12] is not taken into account in our perturbation calculations, by normalizing the values from the perturbation theory to the maximum probability from the TDSE, we can see a good agreement of results from these two theories. The temporal analysis of the populations in the vibrational states (Fig. 6) clearly exhibits the destructive and constructive interference effects for the subsequent pulses in the train for the spectral phase modulation of a dark pulse (left-hand column) and a bright pulse (right-hand column).

To summarize, we have presented a temporal analysis of two-photon coherent control for the excitation to a dissociative state and to bound states in a diatomic molecular model system. We have considered the interaction of these molecular models with spectral phase modulated pulses, which in the temporal domain are represented by a train of pulses. In the case of a two-photon transition to a dissociative state our results have shown that the excitation probability cannot be controlled because of the nuclear dynamics in between subsequent subpulses in the train. In contrast for a two-photon excitation to bound states, the wave packets generated by the subsequent pulses can interfere destructively or constructively depending on the time delay and the CEP difference.

This work was supported by the US Department of Energy.

[1] P. Brumer and M. Shapiro, Chem. Phys. Lett. **126**, 541 (1986).
[2] D. J. Tannor and S. A. Rice, J. Chem. Phys. **83**, 5013 (1985).
[3] D. J. Tannor, R. Kosloff, and S. A. Rice, J. Chem. Phys. **85**, 5805 (1986).
[4] S. A. Rice and M. Zhao, *Optical Control of Molecular Dynamics* (Wiley-Interscience, New York, 2000), Chap. 4.5.
[5] A. M. Weiner, Opt. Commun. **284**, 3669 (2011).
[6] D. Meshulach and Y. Silberberg, Nature (London) **396**, 239 (1998).
[7] N. Dudovich, B. Dayan, S. M. Gallagher Faeder, and Y. Silberberg, Phys. Rev. Lett. **86**, 47 (2001).
[8] P. Panek and A. Becker, Phys. Rev. A **74**, 023408 (2006).
[9] A. Gandman, L. Chuntonov, L. Rybak, and Z. Amitay, Phys. Rev. A **75**, 031401(R) (2007).
[10] T. Bayer, M. Wollenhaupt, C. Sarpe-Tudoran, and T. Baumert, Phys. Rev. Lett. **102**, 023004 (2009).
[11] S. H. Chen, A. Jaroń-Becker, and A. Becker, Phys. Rev. A **82**, 013414 (2010).
[12] D. Meshulach and Y. Silberberg, Phys. Rev. A **60**, 1287 (1999).
[13] M. M. Salour and C. Cohen-Tannoudji, Phys. Rev. Lett. **38**, 757 (1977).
[14] R. Teets, J. Eckstein, and T. W. Hänsch, Phys. Rev. Lett. **38**, 760 (1977).